Effect of diffusion in one-dimensional discontinuous absorbing phase transitions

Carlos E. Fiore[1,*] and Gabriel T. Landi[2,†]
[1]*Instituto de Física, Universidade de São Paulo, Caixa Postal 66318, 05315-970 São Paulo, São Paulo, Brazil*
[2]*Universidade Federal do ABC, 09210-580 Santo André, Brazil*

(Received 4 July 2014; published 18 September 2014)

It is known that diffusion provokes substantial changes in continuous absorbing phase transitions. Conversely, its effect on discontinuous transitions is much less understood. In order to shed light in this direction, we study the inclusion of diffusion in the simplest one-dimensional model with a discontinuous absorbing phase transition, namely, the long-range contact process (σ-CP). Particles interact as in the usual CP, but the transition rate depends on the length ℓ of inactive sites according to $1 + a\ell^{-\sigma}$, where a and σ are control parameters. The inclusion of diffusion in this model has been investigated by numerical simulations and mean-field calculations. Results show that there exists three distinct regimes. For sufficiently low and large σ's the transition is, respectively, always discontinuous or continuous, independently of the strength of the diffusion. On the other hand, in an intermediate range of σ's, the diffusion causes a suppression of the phase coexistence leading to a continuous transition belonging to the directed percolation universality class.

DOI: 10.1103/PhysRevE.90.032123 PACS number(s): 05.70.Ln, 05.50.+q, 05.65.+b

I. INTRODUCTION

Discontinuous absorbing phase transitions in low dimensions have attracted a great deal of interest in recent years [1–7]. Much of this effort has been based on the fundamental problem of determining the necessary ingredients for their occurrence. Generically, discontinuous transitions require an effective mechanism that suppresses the formation of absorbing minority islands (within the active phase) induced by fluctuations. Although they may occur in larger dimensions, there is strong evidence that in one dimension short-range interactions cannot stabilize compact clusters [4]. In contrast, a long-range counterpart of the contact process (CP), named σ-CP [5], has revealed such occurrence, even in one dimension. In the σ-CP, particles are created and annihilated like in the usual short-range CP [1], but the creation rate depends on the length ℓ of the island of inactive sites according to the expression $1 + a\ell^{-\sigma}$. For small σ the interactions are effectively long range leading to a discontinuous transition [5]. This can be understood by noting that the long-range interaction introduces a collective behavior that is able to suppress the formation of minority islands. On the other hand, when σ is large the phase transition becomes continuous and belongs to the directed percolation (DP) universality class, in similarity with the usual CP. Hence there exists a tricritical point σ_t where the transition changes from discontinuous to continuous.

It is known that the presence of certain dynamics, such as disorder and diffusion, may drastically change the critical behavior and the classification of the phase transition. As in the equilibrium case, disorder may induce distinct universality classes and Griffiths phases [1,8–10]. Particle diffusion, on the other hand, can also be responsible for substantial changes, including not only the emergence of distinct universality classes [9] but also the appearance of novel structures in the phase diagrams [11]. However, much of the effort on understanding the role of these ingredients has focused on continuous transitions, with the situation for discontinuous transitions being much less understood [12].

In order to shed some light in this direction, we analyze the role of diffusion in the σ-CP model, which is perhaps the simplest one-dimensional system presenting a discontinuous absorbing transition. This has been accomplished using numerical simulations performed in both the constant rate (ordinary) [1] and the constant particle number (conserved) ensembles [13–16]. The simulations were performed for several values of the diffusion rate and several values of σ. We have found that the tricritical point σ_t (which signals the crossover from continuous to discontinuous transition) decreases as the diffusion increases. This leads to three distinct scenarios. For sufficiently small and large values of σ, the diffusion does not change the phase transition, remaining always discontinuous and continuous, respectively. On the other hand, in an intermediate range of σ's, the diffusion causes a suppression of the phase coexistence leading to a continuous transition belonging to the DP universality class. The problem is also studied using mean-field theory in the pair approximation. As we show, however, mean-field calculations do not agree with the numerical results: they predict that σ_t should increase with D and not the inverse. The reasons for this discrepancy are discussed.

This paper is organized as follows: In Sec. II we present the model and in Sec. III the mean-field results. Numerical results are presented in Sec. IV and in Sec. V we draw the conclusions.

II. MODEL

The one-dimensional diffusive σ-CP [5] is defined as follows. To each site i of a one-dimensional lattice we associate an occupation variable η_i that takes the values 0 or 1 according to whether the site is empty or occupied. The dynamics involves three processes: spontaneous annihilation of a single particle (schematically represented by $1 \to 0$), catalytic creation of a particle ($0 \to 1$), and particle hoppings to a nearest-neighbor empty site ($01 \to 10$ or $10 \to 01$). The transition rate w_i is given by the following expression:

$$w_i = Dw^D_{i,i+1} + (1 - D)\big(\alpha w^a_i + w^c_i\big), \qquad (1)$$

*fiore@if.usp.br
†gtlandi@gmail.com

where D and α are the diffusion and annihilation rates, respectively, and $w^D_{i,i+1}$, w^a_i, and w^c_i represent the diffusion, annihilation, and creation processes, respectively. Their expressions are given by $w^D_{i,i+1} = \eta_i\bar{\eta}_{i+1} + \bar{\eta}_i\eta_{i+1}$ (where $\bar{\eta}_i = 1 - \eta_i$), $w^a_i = \eta_i$, and

$$w^c_i = \frac{1}{2}\sum_{\ell=1}^{\infty}(1 + a\ell^{-\sigma})\{\eta_{i-1}\bar{\eta}_i\bar{\eta}_{i+1}\cdots\bar{\eta}_{i+\ell-1}\eta_{i+\ell} + \eta_{i+1}\bar{\eta}_i\bar{\eta}_{i-1}\cdots\bar{\eta}_{i-\ell+1}\eta_{i-\ell}\}, \tag{2}$$

where a and σ are parameters. When $a = 0$ one recovers the original short-range CP [1,17]. As in that case, single particles are created only in empty sites surrounded by at least one particle. However, in the σ-CP the creation rate depends on the length ℓ between the particles surrounding the empty chosen site.

For large values of α, the system is constrained into the absorbing state, in which no particles are allowed to be created. Decreasing the parameter α, a phase transition to an active state takes place, whose location and classification depends on the parameters a, σ, and D. In order to compare with previous results [5,6,16], we take the value $a = 2$. In this case, when $D = 0$ the crossover regime occurs at $\sigma_t = 1.0(1)$; i.e., the transition is continuous for $\sigma > 1$ (belonging to the DP universality class) and discontinuous for $0 < \sigma < 1$.

III. MEAN-FIELD RESULTS

Here we present a mean-field analysis of the σ-CP with diffusion. Let $f(\eta)$ be an arbitrary function of the vector $\eta = (\eta_1,\eta_2,\ldots)$ and define $\eta^i = (\eta_1,\eta_2,\ldots,\bar{\eta}_i,\ldots)$ and $\eta^{i,j} = (\eta_1,\eta_2,\ldots,\bar{\eta}_i,\ldots,\bar{\eta}_j,\ldots)$. From the underlying master equation it can be shown that the equation governing the time evolution of $\langle f\rangle$ is

$$\frac{df}{dt} = \sum_{i=1}^{N}\{D\langle[f(\eta^{i,i+1}) - f(\eta)]\omega^D_{i,i+1}\rangle + (1 - D)\langle[f(\eta^i) - f(\eta)][\omega^c_i + \alpha\omega^a_i]\rangle\}, \tag{3}$$

where the first and second terms take into account the particle diffusion and the creation and annihilation subprocesses, respectively.

From Eq. (3) we derive relations from the mean-field approach in the pair approximation. This second-order approximation is required since, in the simple mean field, the diffusion term drops out entirely. Hence, we approximate the probability pertaining to a string of sites by

$$P(\eta_1,\eta_2,\eta_3,\ldots,\eta_\ell) \simeq \frac{P(\eta_1,\eta_2)P(\eta_2,\eta_3)\cdots P(\eta_{\ell-1},\eta_\ell)}{P(\eta_2)P(\eta_3)\cdots P(\eta_{\ell-1})}. \tag{4}$$

Since two equations are required, we chose the system density $\rho = P(1) = \langle\eta_i\rangle$ and the two-site probability $z = P(01) = \langle\bar{\eta}_i\eta_{i+1}\rangle$. Making use of the translation symmetry of the problem it is possible to show that Eq. (3) for $f = \eta_i$ becomes

$$\frac{d\rho}{dt} = (1 - D)\left\{z - \alpha\rho + \frac{az^2}{1-\rho-z}\mathrm{Li}_\sigma\left(\frac{1-\rho-z}{1-\rho}\right)\right\}, \tag{5}$$

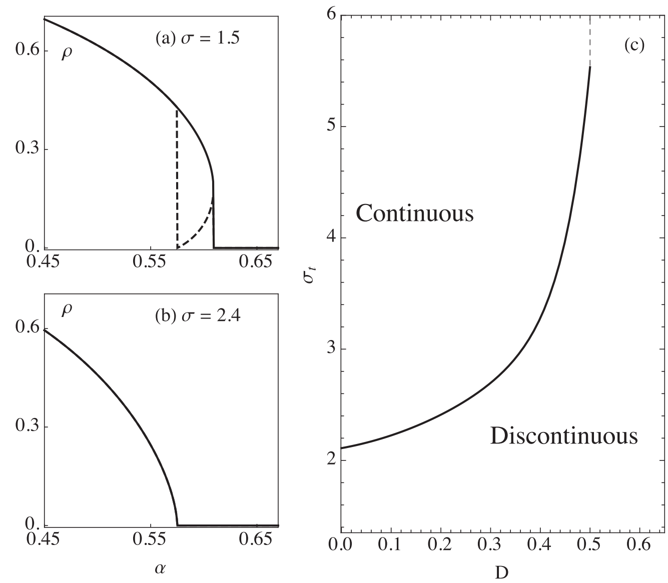

FIG. 1. Mean-field results. (a) and (b) ρ vs α for $a = 2$, $D = 0.15$, and $\sigma = 1.5$ and 2.4. The dashed curve in (a) correspond to the unstable solution. (c) Phase diagram showing the value $\sigma_t(D)$ where the transition changes from continuous to discontinuous. For $D > 0.5$ the transition is always discontinuous.

where Li_σ is the polylog function defined as

$$\mathrm{Li}_\sigma(x) = \sum_{\ell=1}^{\infty}\frac{x^\ell}{\ell^\sigma}.$$

Similarly Eq. (3) for $f = \bar{\eta}_i\eta_{i+1}$ yields

$$\frac{dz}{dt} = (1 - D)\left\{\alpha(\rho - 2z) - \frac{(1+a)z^2}{1-\rho}\right\} + 2D\left\{z - \frac{z^2}{\rho(1-\rho)}\right\}. \tag{6}$$

The steady-state behavior is obtained by setting $d\rho/dt = dz/dt = 0$ in Eqs. (5) and (6), which yields a system of algebraic equations for ρ and z [18].

In resemblance with the van der Waals loop, which signals a discontinuous transition studied under mean-field-like approaches, the phase transitions can be identified by the existence of a spinodal behavior. The coexistence point is estimated by the maximum value of α, whose absence signals a continuous phase transition.

In Figs. 1(a) and 1(b) we exemplify mean-field results for $a = 2$, $D = 0.15$, and distinct σ's. The transition is seen to be discontinuous for $\sigma = 1.5$ and continuous for $\sigma = 2.4$. The complete phase diagram is shown in Fig. 1(c) along with the tricritical line $\sigma_t(D)$ that separates continuous from discontinuous transitions. We see that σ_t increases monotonically with D until $D = 0.5$. Above this point the transition is always discontinuous. This monotonic increase of $\sigma_t(D)$ with D, as will be seen below, is in disagreement with the numerical simulations. The reasons for this will be discussed in Sec. V.

IV. NUMERICAL RESULTS

We now present the numerical simulations of the diffusive σ-CP model. For completeness, and in order to obtain a global picture, we perform simulations in both the constant particle number ensemble and the constant rate ensemble.

A. Constant particle number ensemble

In the constant particle number (conserved) ensemble, the total particle number n is held fixed and both creation and annihilation processes are replaced by just one jump process. Letting w_{ij} be the transition rate denoting the jump from a particle at i to an empty site j, we have that

$$w_{ij} = w_i^a w_j^c. \tag{7}$$

This jump process can be viewed as the annihilation of a particle in site i and the creation in site j. In Refs. [14,15,19,20] it has been shown that the mean annihilation rate $\bar{\alpha}$ is given by

$$\bar{\alpha} = \frac{\langle w_j^c \rangle_c}{\langle w_i^a \rangle_c}, \tag{8}$$

where $\langle \cdots \rangle_c$ denotes the average of a given quantity in this ensemble. Note that the above expression for the average $\bar{\alpha}$ is equivalent to the expression $\langle \omega_j^c \rangle = \alpha \langle w_j^a \rangle$ obtained for the constant rate ensemble in the steady regime.

An advantage of using the conserved ensemble is that, in this version the σ-CP does not have, strictly speaking, an absorbing state (in contrast to the constant rate ensemble), except the trivial case $n = 0$. Another advantage is that both the transition point and the classification of the transition are readily obtained by performing numerical simulations for distinct n's in the subcritical regime. According to Broker and Grassberger [21] and afterwards [13,16,20], the addition of particles placed in an infinite lattice drives the system toward the transition point α_0 according to the expression [13,16,21]

$$\bar{\alpha} - \alpha_0 \sim n^{-1}. \tag{9}$$

Thus, we may locate the transition point by linearly extrapolating $1/n$ (note that n is held fixed but the system density $\rho \to 0$).

The classification of the phase transition is obtained by measuring the particle displacements for different n. Letting R be the mean distance between the particles located at the extremities of the system, we have that [1,16,20]

$$R \sim n^{1/d_F}, \tag{10}$$

where d_F is the fractal dimension. For one-dimensional systems belonging to the DP universality class, the clusters are fractals with fractal dimension $d_F = 0.747\,92\ldots$ [22], whereas at the phase coexistence it is the proper Euclidean dimension $d = 1$, consistent with the emergence of a compact cluster. Hence, the order of the transition may be inferred by analyzing the slope of $\ln R$ vs $\ln n$.

The actual numerical simulation in the conserved ensemble is realized as follows. With probability D a randomly chosen particle hops to its nearest-neighbor site (provided it is empty), whereas with probability $1 - D$ the jumping process is chosen instead. In this case an occupied site is chosen at random. If its neighbor is empty, we occupy it with probability $p_\ell = (1 + a\ell^{-\sigma})/(1 + a)$, where ℓ is the length of the island of inactive sites in which the active site is located. The constant factor $1/(1 + a)$ is used in order to guarantee that $p_\ell \leqslant 1$. The particle that occupies the empty site is also chosen at random, thus conserving the total particle number n.

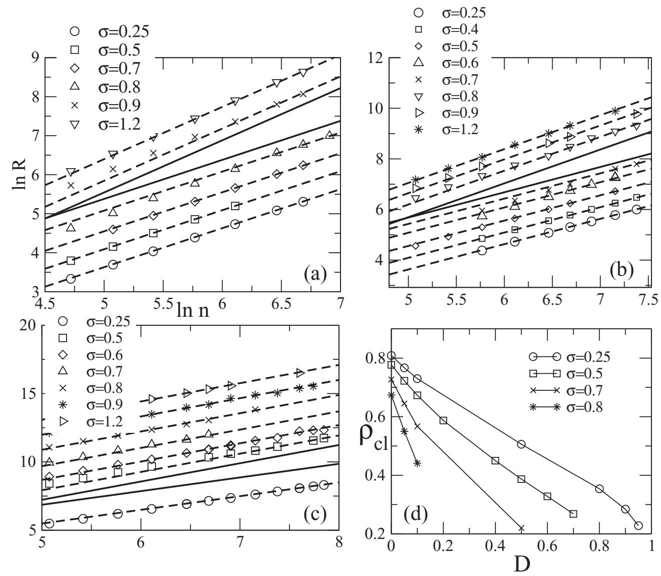

FIG. 2. Log-log plot of the maximum distance R vs the particle number n for distinct values of σ and for $D = 0.1$ (a), 0.5 (b), and 0.95 (c). The upper and lower straight lines have slopes $1/d_F = 1.337\ldots$ and 1, respectively [cf. Eq. (10)]. In (d) we plot the cluster density $\rho_{\rm cl}$ vs D, at the phase coexistence, for distinct values of σ.

In Fig. 2 we show results for $D = 0.1$, 0.5, and 0.95 and distinct values of σ. For $D = 0.1$ [Fig. 2(a)] the phase transition is discontinuous for $0 < \sigma < 0.9$ and continuous for $\sigma \geqslant 0.9$. This is close to the case $D = 0$, in which the crossover occurs at $\sigma_t = 1.0(1)$ [5,16]. The cases $D = 0.5$ and 0.95 exhibit a similar behavior. However, the effect of diffusion is now more pronounced with the crossover occurring at $\sigma_t = 0.75(5)$ and 0.45(5), respectively. Inspection of the cluster density $\rho_{\rm cl} = n/R$ (at the phase coexistence) shown in Fig. 2(d) reveals that the particle clusters become less compact as D increases.

The values of the tricritical line $\sigma_t(D)$ are summarized in Fig. 3, where the monotonically decreasing behavior is clearly observed. This is in stark disagreement with the mean-field predictions of Fig. 1(c), in which $\sigma_t(D)$ grows with D. The reasons for this discrepancy will be discussed below.

All these results are found to be similar to those obtained in Ref. [6], in which distinct interaction rules have been considered in order to study the phase coexistence by "weakening" the long-range interaction. [23]. Thus, the above results suggest that the diffusion also "weakens" the long-range interaction, in similarity to Ref. [6]. As a consequence, in a high diffusion regime, the phase coexistence yields only for sufficiently lower σ's. Since the tricritical line $\sigma_t(D)$ is a decreasing function of D, when $\sigma > 1$ the role of the diffusion is irrelevant with respect to the change in the order of the transition. In other words, the diffusion does not shift the phase transition, remaining continuous for all values of $\sigma > 1$. This can be understood by recalling that, when σ is large, the

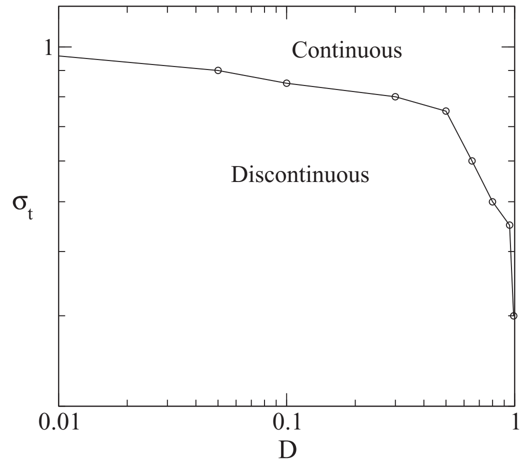

FIG. 3. The tricritical line $\sigma_t(D)$ obtained from numerical simulations (cf. Fig. 2).

long-range factor $1 + a\ell^{-\sigma}$, responsible for the occurrence of a phase coexistence, decays rapidly with ℓ, becoming closer to the short-range value 1. Since in this case the phase transition is continuous for all diffusion rates [3], the conclusion follows.

B. Constant rate ensemble

In order to confirm the above conclusions, we have also performed numerical simulations in the constant rate ensemble. Unlike the conserved ensemble, the creation and annihilation rates are the control parameters, whereas the particle density is a fluctuating quantity. To locate the transition point α_0 and classify the transition, we perform spreading simulations starting from an initial configuration with a single particle at the origin. The proper quantities to evaluate are the survival probability $P_s(t)$, the mean particle number $N(t)$, and the mean square displacement $R^2(t)$. At the transition point they follow power-law behaviors given by

$$P_s(t) \sim t^{-\delta}, \quad N(t) \sim t^{\eta}, \quad R^2(t) \sim t^{2/z}, \tag{11}$$

where δ, η, and z are associated dynamic critical exponents. For continuous transitions belonging to the DP universality class these exponents present the well-known values

$$\delta = 0.159\,464(6), \quad \eta = 0.313\,686(8), \quad z = 1.580\,745(10). \tag{12}$$

Instead, at the one-dimensional phase coexistence (despite the order-parameter gap) their values read [9,10]

$$\delta = 1/2, \quad \eta = 0, \quad z = 1. \tag{13}$$

Hence, the order of the phase transition can be obtained from the values of these critical exponents.

This analysis is also useful since it allows one to draw a comparison with results obtained from the conserved ensemble, whose above dynamic exponents and fractal dimension d_F are related through the expression $d_F = 2(\eta + \delta)/z$. Away from the critical point, all quantities deviate from power-law behaviors, reaching a regime of endless activity for $\alpha < \alpha_0$ and exponential decay toward extinction for $\alpha > \alpha_0$. The continuous transitions have also been confirmed by studying the time decay of the system density ρ starting from a fully

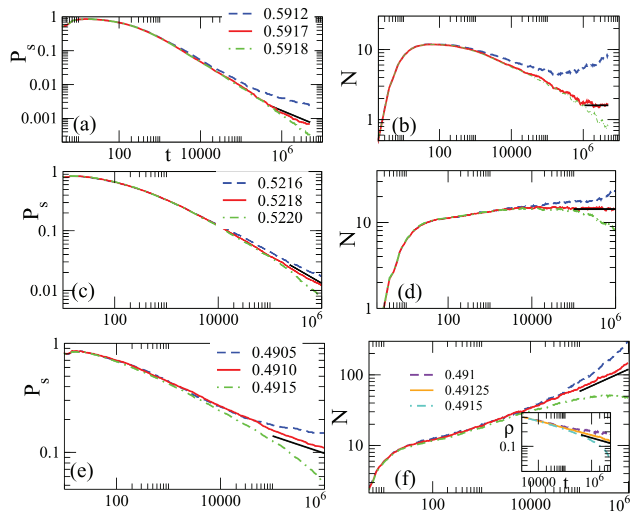

FIG. 4. (Color online) The time evolution of $P_s(t)$ and $N(t)$ in the constant rate ensemble for distinct values of α and $D = 0.1$. (a) and (b) $\sigma = 0.25$; (c) and (d) $\sigma = 0.8$; (e) and (f) $\sigma = 1.2$. The slopes of the black straight lines are given by Eq. (13) for (a)–(d) and Eq. (12) for (e) and (f). The inset in image (f) shows the decay of the density ρ and the black line has slope $\theta = 0.159\,464(6)$.

occupied initial configuration. At the critical point it behaves as $\rho(t) \sim t^{-\theta}$, where for the CP $\theta = \delta = 0.159\,464(6)$. In contrast, in the active and absorbing phases, $\rho(t)$ converges to a well-defined value $\bar{\rho} \neq 0$ and vanishes exponentially, respectively. For the evaluation of ρ, we have considered $L = 20\,000$ and averages have been evaluated over 30 000 initial configurations.

The main results for the constant rate ensemble are shown in Figs. 4–6 for $D = 0.1$, 0.5, and 0.95, respectively. In each figure we plot both $P_s(t)$ and $N(t)$ for three distinct values of σ; namely, 0.25, 0.8, and 1.2. In all cases, the above quantities have been calculated over 30 000 initial

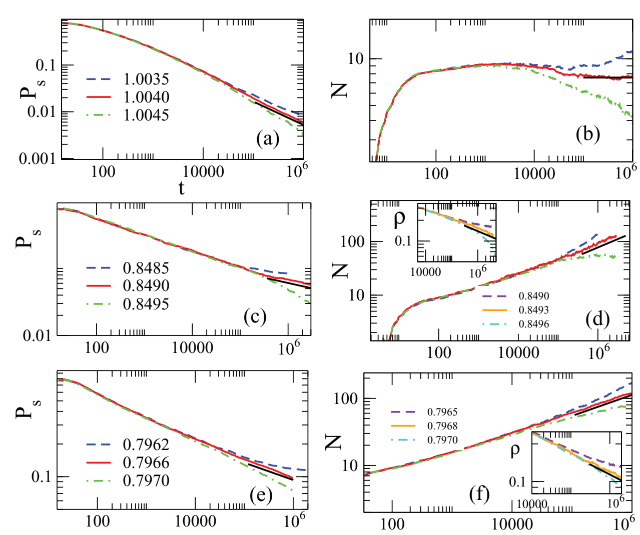

FIG. 5. (Color online) Same as Fig. 4 but for $D = 0.5$. The slopes of the black straight lines are given by Eq. (13) for (a) and (b) and Eq. (12) for (c)–(f). The insets show the time decay of ρ for distinct α's and the black lines have slope $\theta = 0.159\,464(6)$.

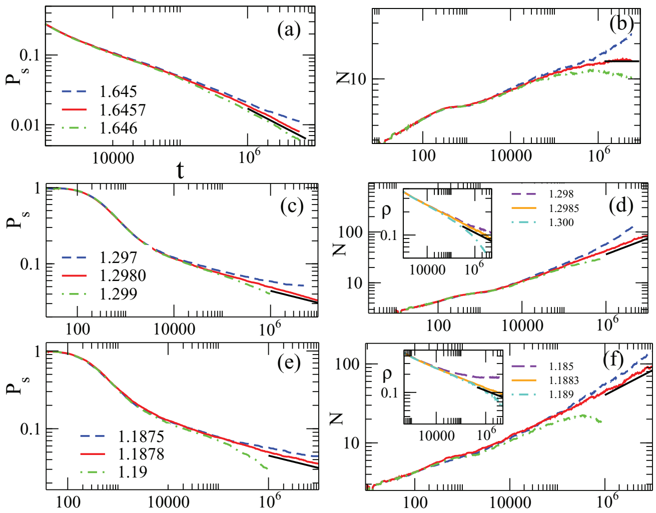

FIG. 6. (Color online) Same as Fig. 5 but for $D = 0.95$. The slopes of the black straight lines are given by Eq. (13) for (a) and (b) and Eq. (12) for (c)–(f). The insets show the time decay of ρ for distinct α's and the black lines have slope $\theta = 0.159\,464(6)$.

configurations. In Fig. 4 we show the main results for $D = 0.1$. When $\sigma = 0.25$ and 0.8 [Figs. 4(a)–4(d)], we observe an algebraic behavior with the exponents $\delta = 1/2$ and $\eta = 0$ of Eq. (13) [see also Eq. (11)]. This signifies, in agreement with Fig. 2, a discontinuous transition. On the other hand, for $\sigma = 1.2$ [Figs. 4(e) and 4(f)] the power-law regime has the DP exponents of Eq. (12), indicating a continuous transition. The time decay of ρ, shown in the inset of Fig. 4(d), confirms the algebraic behavior with the DP exponent. The analysis is repeated in Figs. 5 and 6 for $D = 0.5$ and 0.95. In both cases the phase transition is discontinuous for $\sigma = 0.25$ and continuous for $\sigma = 0.8$ and 1.2, in agreement with results from the conserved ensemble and thus confirming that σ_t decreases by raising D. Analysis of the time decay of ρ reinforces this result. The middle curves in the inset present algebraic decays consistent with the DP values $\theta = 0.159\,464(6)$ at α's very close to the α_0. In fact, these estimates are somewhat larger than α_0, due to finite size effects.

Hence, we conclude that the results of the constant rate ensemble are in complete agreement with those of the conserved ensemble. In contrast with mean-field results, the value σ_t, where the order of the transition changes, diminishes with increasing diffusion.

V. DISCUSSION AND CONCLUSION

In this paper we have investigated the role of diffusion in the simplest model presenting a discontinuous phase transition with an absorbing state. It is a counterpart of the usual contact process, in which the particle creation rate depends on the length ℓ of inactive islands surrounding the creation site according to $1 + a\ell^{-\sigma}$. In the absence of diffusion, a tricritical point σ_t separates discontinuous from continuous transition. For $a = 2$ this point occurs at $\sigma_t = 1.0(1)$.

We investigated, by means of numerical simulation and mean-field calculations, the effect of diffusion on the phase coexistence regimes and crossover σ_t. Results for distinct values of σ and diffusion rates showed that the crossover σ_t is monotonically reduced as the diffusion increases, similarly to the interactions introduced to weaken the long-range feature studied in Ref. [6]. This suggests that by increasing the diffusion toward the limit $D \to 1$, only sufficient small σ are able to stabilize compact clusters. In fact, results for $D = 0.99$ (cf. Fig. 3) show that for sufficiently low σ ($\sigma \leqslant 0.2$), the transition is still discontinuous, but the value $\sigma_t \sim 0.3$ signals the emergence of a continuous transition. Hence, our results reveal a novel role played by the diffusion in phase transitions, being responsible for weakening the compact displacement among the particles. Notwithstanding, we emphasize that further studies of discontinuous absorbing transitions in the presence of diffusion are necessary in order to yield a complete picture of the problem.

Finally, we turn to the marked disagreement between the mean-field results and the numerical simulations, regarding the dependence of σ_t on D. As we have seen, in the mean-field approximation σ_t was found to be a monotonically increasing function of D, whereas in the numerical simulations the exact opposite behavior was observed. Moreover, in the mean field we have found that above $D = 0.5$ the transition should be discontinuous for any value of σ. We attribute this disagreement to the correlations neglected by the mean-field theory, which become more important in low dimensions (as in the present case). In fact a similar disagreement between mean-field and numerical simulations in a one-dimensional discontinuous transition has been recently investigated in Ref. [24]. Another possibility concerns the restrictions of the lattice particle occupations (only one particle can occupy a given site) that, together with the present lattice topology, could prevent the particle clustering induced by increasing the diffusion. In other words, a lattice model allowing multiple occupation of each site may lead to results compatible with mean-field predictions. We remark that, notwithstanding, all these points deserve further investigations.

ACKNOWLEDGMENT

C.E.F. acknowledges the financial support from CNPQ under Grant No. 307431/2012-6 and G.T.L. acknowledges the support from FAPESP under Grant No. 2014/01218-2.

[1] J. Marro and R. Dickman, *Nonequilibrium Phase Transitions in Lattice Models* (Cambridge University Press, Cambridge, England, 1999).
[2] R. M. Ziff, E. Gulari, and Y. Barshad, Phys. Rev. Lett. **56**, 2553 (1986).
[3] C. E. Fiore and M. J. de Oliveira, Phys. Rev. E **70**, 046131 (2004).
[4] H. Hinrichsen, arXiv:cond-mat/0006212.
[5] F. Ginelli, H. Hinrichsen, R. Livi, D. Mukamel, and A. Politi, Phys. Rev. E **71**, 026121 (2005).

[6] C. E. Fiore and M. J. de Oliveira, Phys. Rev. E **87**, 042101 (2013).
[7] C. E. Fiore, Phys. Rev. E **89**, 022104 (2014).
[8] See, for example, T. Vojta and M. Dickison, Phys. Rev. E **72**, 036126 (2005); H. Barghathi and T. Vojta, Phys. Rev. Lett. **109**, 170603 (2012).
[9] M. Henkel, H. Hinrichsen, and S. Lubeck, *Non-Equilibrium Transitions* (Springer, New York, 2008), Vol. 1.
[10] G. Odor, Rev. Mod. Phys **76**, 663 (2004).
[11] R. Dickman, Phys. Rev. B **40**, 7005 (1989).
[12] P. Villa Martín, J. A. Bonachela, and M. A. Muñoz, Phys. Rev. E **89**, 012145 (2014).
[13] T. Tomé and M. J. de Oliveira, Phys. Rev. Lett. **86**, 5643 (2001).
[14] H. J. Hilhorst and F. van Wijland, Phys. Rev. E **65**, 035103 (2002).
[15] M. J. de Oliveira, Phys. Rev. E **67**, 027104 (2003).
[16] C. E. Fiore and M. J. de Oliveira, Phys. Rev. E **76**, 041103 (2007).
[17] T. E. Harris, Ann. Probab. **2**, 969 (1974).
[18] It is possible to solve Eq. (6) for z as a function of ρ and then insert this result into Eq. (5). This has the advantage of yielding a single algebraic equation for ρ as a function of the parameters a, D, σ, and α, which is much simpler to solve numerically than a system of two coupled equations.
[19] E. S. Loscar and E. V. Albano, Phys. Rev. E **65**, 066101 (2002).
[20] C. E. Fiore and M. J. de Oliveira, Phys. Rev. E **72**, 046137 (2005).
[21] H.-M. Bröker and P. Grassberger, Physica A **267**, 453 (1999).
[22] T. Vicsek, *Fractal Growth Phenomena*, 2nd ed. (World Scientific, Singapore, 1992).
[23] The procedures to weaken the long-range interaction were to decrease the long-range parameter a and the introduction of a competition with short-range interactions. More details can be seen in Ref. [6].
[24] G. Ódor and R. Dickman, J. Stat. Mech. (2009) P08024.